Published in final edited form as:
J Comp Neurol. 2010 July 1; 518(13): 2525–2537. doi:10.1002/cne.22350.

An extra-cerebellar role for *cerebellin1*: modulation of dendritic spine density and synapses in striatal medium spiny neurons

S. V. Kusnoor[1], **J. Parris**[2], **E. C. Muly**[3], **J. I. Morgan**[2], and **A. Y. Deutch**[1,*]

[1]Program in Neuroscience and Departments of Psychiatry and Pharmacology Vanderbilt University Medical Center Nashville, TN 37212 USA

[2]Department of Developmental Neurobiology St. Jude Children's Research Hospital Memphis, TN 38105 USA

[3]Department of Psychiatry and Behavioral Sciences Emory University School of Medicine 30322 USA and Division of Neuroscience, Yerkes Primate Research Center, Atlanta GA 30322 USA and Atlanta Department of Veterans Affairs Medical Center Decatur, GA USA

Keywords

Cbln1; *dopamine*; *intralaminar*; *parafascicular nucleus*; *thalamostriatal*

Cerebellin1 (Cbln1) is a secreted glycoprotein that was originally isolated from the cerebellum and subsequently found to regulate synaptic development and stability. Cbln1 has a heterogeneous distribution in brain, but the only site in which it has been shown to have central effects is the cerebellar cortex, where loss of Cbln1 causes a reduction in granule cell-Purkinje cell synapses. Neurons of the thalamic parafascicular nucleus (PF), which provide glutamatergic projections to the striatum, also express high levels of Cbln1. We first examined Cbln1 in thalamostriatal neurons and then determined if *cbln1* knockout mice exhibit structural deficits in striatal neurons. Virtually all PF neurons expressed Cbln1-immunoreactivity (-ir). In contrast, only rare Cbln1-ir neurons are present in the central medial complex, the other thalamic region that projects heavily to the dorsal striatum. In the striatum Cbln1-ir processes are apposed to medium spiny neuron (MSN) dendrites; ultrastructural studies revealed that Cbln1-ir axon terminals form axodendritic synapses with MSNs. Tract tracing studies found that all PF cells retrogradely-labeled from the striatum express Cbln1-ir. We then examined the dendritic structure of Golgi-impregnated MSNs in adult *cbln1* knockout mice. MSN dendritic spine density was markedly increased in *cbln1*$^{-/-}$ mice relative to wildtype littermates, but total dendritic length was unchanged. Ultrastructural examination revealed an increase in the density of MSN axospinous synapses in *cbln1*$^{-/-}$ mice, with no change in PSD length. Thus, Cbln1 determines the dendritic structure of striatal MSNs, with effects distinct from those seen in the cerebellum.

Precerebellin (Cbln1) was originally isolated as the precursor of a cerebellar peptide cerebellin (Slemmon et al., 1984) and was subsequently shown to define a subfamily (Cbln1–4) of the C1q/TNFα superfamily of proteins (Urade et al., 1991; Pang et al., 2000; Bao et al., 2005). Cbln1 is secreted as homo- and hetero-trimeric complexes from granule cells (Pang et al., 2000; Bao et al., 2005, 2006; Wei et al., 2007), and is essential for maintaining the structure and function of parallel fiber–Purkinje cell (pf-PC) synapses (Hirai et al., 2005). *Cbln1* null mutant mice have a decreased number of pf-PC synapses, with

*Correspondence: Psychiatric Hospital at Vanderbilt, Suite 3066 1601 23rd Ave South Nashville TN 37212 Tel (615) 327-7080 ariel.deutch@vanderbilt.edu.

many Purkinje cell dendritic spines lacking a presynaptic partner (Hirai et al., 2005; Ito-Ishida et al., 2008). These morphological changes are associated with an absence of long-term depression at pf-PC synapses and gross ataxia (Hirai et al., 2005). A recent report noted that the injection of recombinant Cbln1 into the subarachnoid space of *cbln1*$^{-/-}$ mice transiently restores synapse number in the cerebellar cortex (Ito-Ishida et al., 2008).

Despite its name, Cbln1 has a widespread but heterogeneous distribution in the brain (Mugnaini and Morgan, 1987; Miura et al., 2006; Wei et al., 2007). Among the sites with abundant central expression of *cbln1* mRNA and protein is the thalamic parafascicular nucleus (PF; Miura et al., 2006; Murray et al., 2007; Wei et al., 2007). Thalamostriatal neurons originate in the PF and in the more rostrally-situated central medial, paracentral, and centrolateral cluster of neurons (CM complex) of the rat. These neurons provide dense glutamatergic projections to the striatum, where they synapse with medium spiny neurons (MSNs) and certain interneurons (Dube et al., 1988; Berendse and Groenewegen, 1990; Lapper and Bolam, 1992; Smith et al., 2004). Although historically thalamostriatal axons were viewed as synapsing onto the dendritic shaft of MSNs, it is now clear that many PF-derived axons synapse with MSN dendritic spines (Sadikot et al., 1992; Lacey et al., 2007). The functional significance of thalamostriatal neurons is not fully understood (Giménez-Amaya et al., 2000; Matsumoto et al., 2001; Minamimoto et al., 2002, 2009; Smith et al., 2009). Recent studies have focused on interactions between the glutamatergic thalamostriatal neurons and the dopamine innervation of the striatum (Bacci et al., 2004; Ding et al., 2008; Smeal et al., 2008; Lanciego et al., 2009; Smith et al., 2009).

In view of the high density of Cbln1-expressing cells in the PF, we examined the localization of Cbln1 in the thalamostriatal system and determined if the synaptic organization of striatal MSNs is altered in *cbln1* null mutant mice.

Materials and Methods

Animals

cbln1$^{-/-}$ mice and their wildtype littermates (Hirai et al., 2005), between 3 and 5 months of age, were group housed with food and water freely available. The *cbln1*$^{-/-}$ mice were backcrossed to the C57Bl/6J strain for more than nine generations. Sprague-Dawley rats (Harlan Sprague-Dawley; Indianapolis, IN) were group housed with food and water available *ad libitum*. All studies were performed in accordance with the National Institutes of Health Guide for Care and Use of Laboratory Animals and under the oversight of the institutional Animal Care and Use Committee.

Antibody Characterization

A table showing the antibodies used, the sources of these antibodies, and the immunogen against which the antibodies were generated is shown in Table 1. In immunoblots of mouse cerebellar extracts, the Cbln1 antibody detected a 35 kDa band, which corresponds with the molecular weight of full-length Cbln1, as well as several lower molecular weight bands that are thought to be degradation products (Bao et al. 2005). A complete loss of Cbln1-ir bands was observed in immunoblots of mouse cerebellar extracts from the cbln1 null mutant mouse (Bao et al. 2006). Preadsorbtion of the Cbln1 antibody with excess immunogen prevents staining in tranfected HEK293 cells and eliminates Cbln1 bands on immunoblots of adult mouse cerebellar extracts (Bao et al. 2005). The antibody is specific for Cbln1 and does not stain any bands of gels loaded with protein from HEK293 cells transfected with Cbln2, Cbln3, or Cbln4 (Bao et al. 2005). Under immunohistochemical conditions the Cbln1 antibody does not result in any specific staining in the cerebellum of the *cbln1* knockout

mouse (Wei et al. 2009), and as shown in Figure 2, the antibody does not detect Cbln1-ir cells in the thalamus of the cbln1$^{-/-}$ mouse.

The NeuN antibody recognizes two bands at ~46–48 kDa that agree with its deduced mass, according to the manufacturer (Millipore, Billerica, MA). The antibody stained a pattern of larger, neuronal nuclei that was consistent with previous reports (Mullen et al. 1992).

Preadsorption of the cholera toxin B antibody (List Biological, Campbell, CA) with excess choleragenoid blocks immunolabeling (Stocker et al. 2006). The antibody does not stain tissue from animals that were not injected with cholera toxin B (Pakan et al. 2008).

The vesicular glutamate transporter 2 (VGluT2) antibody detects a band at ~66 kDa in immunoblots of mouse brain, which is consistent with its molecular weight (see Figure 6) and a second band at ~36 kDa. As reported by the manufacturer (MAb Technologies, Inc.), preabsorption of the antibody with the VGluT2 peptide immunogen blocks the detection of the 66 kDa band, but preabsorption with VGluT1 does not alter labeling of this band. The antibody stains rat and mouse brain in a pattern that is consistent with previous reports (Kaneko et al. 2002;Fujiyama et al. 2006; Mathur and Deutch 2008).

Immunohistochemistry

Animals were perfused with 0.1M phosphate-buffered saline followed by 4% paraformaldehyde in phosphate buffer, and immunohistochemistry was used to localize Cbln1-immunoreactivity (-ir) using our previously described methods (Bubser et al., 2000), with the exception that an antigen retrieval method was used to enhance Cbln1 staining. Free-floating sections were incubated in 10 mM sodium citrate buffer containing 0.05% Tween 20 (pH 6.0) at 80°C for 25–30 min, and then washed extensively before the tissue was processed for immunohistochemical localization of Cbln1, using our previously characterized (E3) antibody (see Bao et al., 2005 and Wei et al., 2007).

The software program Neurolucida (MBF Bioscience; Williston, VT) was used to chart the distribution of Cbln1-ir elements in the thalamus and striatum. A Zeiss LSM-510 confocal microscope was used to acquire fluorescent images.

Photomicrographs were subjected to minimal modification using Photoshop, with slight changes in image brightness and contrast. Images were cropped to focus on the most salient part of the original photomicrographs.

Retrograde tracer studies

The retrograde tracer FluoroGold (FG; 3% in 0.1M cacodylate, pH 3.3; Fluorochrome, Denver, CO) was iontophoretically deposited into the dorsolateral striatum of rats through pipettes with tip diameters of 18–25 μm, using pulsed (7s on/7s off) +5.0 mA current for 15 minutes. In three animals 200 nl of Cholera toxin B (List Biological Laboratories; Campbell, CA) was pressure injected into somatomotor cortex of animals that also received striatal FG deposits. Animals were sacrificed 10 days later, and immunohistochemical methods were used to reveal retrogradely-labeled neurons expressing Cbln1-ir in the cortex, thalamus, and midbrain.

Intracellular injections of MSNs

Two adult, male Sprague-Dawley rats were rapidly perfused with 300 ml of 9.25% sucrose at 37° C, followed by 100–150 ml of 4% paraformaldehyde in phosphate buffer. The brains were then removed, postfixed at 4°C for 30 minutes, and 150 μm-thick coronal sections were cut on a vibrating microtome. Striatal cells were iontophoretically filled with 8%

Lucifer Yellow (LY; Sigma-Aldrich, St. Louis, MO) in 50 mM Tris, pH 7.4, using continuous +5.0 nA current for 3–5 minutes. Immunohistochemistry was subsequently used to localize Cbln1 in axons, as described above. The software program Imaris (Bitplane, Saint Paul, MN) was then used to analyze Cbln1 appositions with MSN dendrites.

Golgi impregnation

cbln1 null mutant mice and their wildtype littermates were perfused with 0.1 M phosphate buffer followed by a solution containing 2% paraformaldehyde--2.5% glutaraldehyde in 0.1M phosphate buffer. Coronal sections (150 μm) through the precommissural striatum were cut on a vibrating microtome. The sections were then incubated in 1% osmium tetroxide for 30 minutes and kept in 3.5% potassium dichromate overnight. The next day the sections were developed in 1% silver nitrate for 4–6 hours before being washed extensively, mounted, and coverslipped.

Dendritic analyses of MSNs

Golgi-stained striatal MSNs in the lateral striatum were reconstructed using Neurolucida. Dendritic spine density was determined on segments of secondary or tertiary dendrites at distances between 70 and 90 μm from the soma. Segments from three different dendrites per neuron and 5–6 neurons per animal were analyzed to compute an average dendritic spine density for a given animal. Total dendritic length was also determined.

Dendritic spine length was measured in >50 spines/animal of *cbln1* knockout and wildtype mice. We also determined the shape of dendritic spines in *cbln1*$^{-/-}$ mice, following the classification scheme of Peters and Kaiserman-Abramof (1970).

Ultrastructural studies of striatal MSN dendrites

For electron microscopic localization of Cbln1-ir, animals were sacrificed and perfused with 4% paraformaldehyde, 0.2% glutaraldehyde and 0.2% picric acid in PBS. The brains were blocked and postfixed in 4% paraformaldehyde for 4 hours. For ultrastructural examination of synapses, 2 *cbln1* wildtype and 2 *cbln1* knockout mice were perfused.

Coronal 50 μm thick vibratome sections of the striatum were cut and stored frozen at −80°C in 15% sucrose until immunohistochemical experiments were performed. Single-label immunoperoxidase methods were performed as previously described (Muly et al., 2003), using the rabbit anti-Cbln1 antibody (1:1000). Briefly, sections were thawed, incubated in blocking serum (3% normal goat serum, 1% bovine serum albumin, 0.1% glycine, 0.1% lysine in 0.01 M phosphate buffered saline, pH 7.4) for 1 hour and then placed in primary antiserum diluted in blocking serum. After 36 hours at 4°C, the sections were rinsed and placed in a 1:200 dilution of biotinylated goat anti-rabbit IgG (Jackson Immuno Research, West Grove, PA) for 1 hour at room temperature. The sections were then rinsed, placed in avidin-biotinylated peroxidase complex (ABC Elite, Vector, Burlingame, CA) for 1 hour at room temperature, and then processed to reveal peroxidase using 3,3'-diaminobenzidine (DAB) as the chromagen. Sections were then post-fixed in osmium tetroxide, stained *en bloc* with uranyl acetate, dehydrated, and embedded in Durcupan resin (Electron Microscopy Sciences, Fort Washington, PA). Selected regions of the dorsal striatum were mounted on blocks, and ultrathin sections were collected onto pioloform-coated slot grids and counterstained with lead citrate. Control sections processed as above except for the omission of the primary immunoreagent, did not contain DAB label upon electron microscopic examination.

Ultrathin sections were examined with a Zeiss EM10C electron microscope and immunoreactive elements were imaged using a Dualvision cooled CCD camera (1300 ×

1030 pixels) and Digital Micrograph software (version 3.7.4, Gatan, Inc., Pleasanton, CA). The tissue was scanned and every labeled terminal was examined and if a synaptic contact was identified the terminal and postsynaptic element were imaged. Images selected for publication were saved and imported into an image processing program (Canvas 8; Deneba Software, Miami, FL). The contrast was adjusted, and the images were cropped to meet size requirements

From the stained material obtained from the matched *cbln1* knockout and wildtype mice, 50 images from each animal were examined for a total of 1,108 mm^2 for each genotype. Asymmetric synapses were identified and the postsynaptic element was identified as a spine or dendritic shaft. The density of axospinous synapses for wildtype and knockout mice was calculated. In order to determine if differences in the size of postsynaptic densities contributed to observed differences in synaptic density, we measured the length of axospinous synaptic PSDs in each condition (264 for wildtype and 292 for knockout).

Stereological evaluation of PF neuron number

The number of PF neurons in Nissl-stained coronal sections (42 μm) in *cbln1*$^{-/-}$ mice was determined using the optical dissector method (Stereo Investigator; MBF Bioscience).

Immunoblot analyses

The dorsolateral striatum was rapidly dissected from 1.0-mm-thick coronal sections of *cbln1* null mutant mice (N=4) and their wildtype littermates (N=3) and then stored at −80°C. The frozen tissue was sonicated in 300 μL of 2% SDS containing a 1:10,000 dilution of a protease inhibitor cocktail (P8340; Sigma-Aldrich). The appropriate volume of sample buffer (4% SDS, 20% glycerol, 0.12M Tris, 0.01% bromophenol blue, pH 6.8) was added to the homogenates to adjust the protein concentration of each sample to 10 μg/15 μL. The samples were then stored at −80°C.

Striatal protein homogenates (10 μg total protein) were separated using SDS-PAGE and transferred to nitrocellulose membranes. The membranes were stained with 0.2 % Ponceau-S in 1% acetic acid and digitally scanned. The membranes were blocked in 4% milk (in PBS containing 0.2% Tween-20) and incubated in the rabbit anti-VGluT2 antibody (1:4000) overnight at 4°C. The membrane was then rinsed in PBS and incubated in horseradish peroxidase-conjugated donkey anti-rabbit IgG (1:10,000; Jackson Immunoresearch; West Grove, MA) for 2 hours. The membrane was then rinsed in PBS and developed using enhanced chemiluminescence (Perkin Elmer; Waltham, MA). Multiple X-ray film exposures were obtained.

The films were next digitally scanned, and the optical density of the bands was determined using ImageJ. The samples were normalized to the total protein loaded, as assessed by Ponceau S-staining (Aldridge et al., 2008). The mean normalized signal from the wildtype mice was set at 100%, and the *cbln1*$^{-/-}$ data was expressed relative to this value.

Statistical analyses

Data for dendritic spine density and dendritic length was analyzed by t tests. The proportions of different morphological types of spines was analyzed by a Kruskal-Wallis non-parametric ANOVA.

In the ultrastructural studies of MSN synaptic density in *cbln1*$^{-/-}$ mice, the densities of axospinous synapses for both wildtype and knockout mice were calculated. In order to determine if differences in the size of postsynaptic densities contributed to observed

differences, we measured the length of axospinous synaptic PSDs in each condition and compared the means with t tests.

The stereological data as well as the mean values for striatal VGluT2 levels were also analyzed by comparing values from null mutant and wildtype mice by means of t tests.

Results

Cbln1 in thalamostriatal neurons

Essentially all PF cells expressed dense Cbln1-immunoreactivity (see Figures 1 and 2). Cbln1-ir in PF cells was characteristically punctate (Fig. 2), with the soma and most proximal dendrites being stained. In contrast to the PF, only rarely were Cbln1-ir cells observed in the CM complex, including the centrolateral and paracentral nuclei (see Fig. 1). We did not observe any Cbln1-ir in the PF (Figure 2) or any other brain site (data not shown) in *cbln1* knockout mice, validating the specificity of the Cbln1 antibody. All Cbln1-ir cells in the PF expressed the neuronal marker NeuN (Fig. 2).

Virtually all PF cells that were retrogradely-labeled from the striatum expressed Cbln1-ir (see Fig. 3). We also examined several cases (N = 3) involving retrograde tracer deposits into both the lateral striatum and somatomotor cortex, and found that PF neurons innervating the cortex also expressed Cbln1-ir (see Supplemental Figure 1). Some neurons were triple labeled for Cbln1, FG, and cholera toxin B, indicating that these PF cells collateralized to innervate both striatal and cortical projection fields of the PF.

Cbln1 in the striatum

Scattered Cbln1-ir processes were observed in the striatum, with an appreciably greater density of Cbln1-ir processes in the lateral than medial striatum (see Fig. 1). Occasionally, fine-caliber non-varicose Cbln1-ir axons were seen to terminate in pericellular arrays apposed to striatal (NeuN-ir) neurons (Fig. 3), the great majority of which had a soma size (8–17 μm) that corresponds to that of MSNs. We also examined striatal cells that were injected intracellularly with Lucifer Yellow and then processed to reveal Cbln1 immunoreactivity, in which we confirmed that the major target of Cbln1-ir axons was the MSN, with image analysis showing that Cbln1-ir axons were apposed to both dendritic spines and dendritic shafts (see Fig. 3). At the light microscopic level, Cbln1-ir was typically not observed in NeuN-ir striatal neurons (Fig. 3), although rarely what appeared to be Cbln1-ir puncta were seen in cell bodies.

In order to determine if areas other than the PF send Cbln1 projections to the striatum, we examined the brains of animals in which FG was deposited into the lateral striatum and then charted the presence of double-labeled (FG-positive–Cbln1-ir) neurons in the cortex, substantia nigra, and pontine raphe nuclei. There was a dense group of Cbln1-ir cells in the retrosplenial cortex, but we did not observe any retrogradely-labeled Cbln1-ir neurons in this cortical area. Conversely, a significant number of FG-positive cells that did not express Cbln1 was seen lateral to the retrosplenial cortex (see Supplemental Figure 2). Only rarely were Cbln1-ir cells seen in other cortices, and none of these cells was retrogradely labeled. Similarly, we did not see any double-labeled Cbln1-ir--PF-positive cells in dorsal or median raphe (Supplemental Figure 2). In the substantia nigra we observed a single Cbln1-ir neuron in the dorsal tier of the pars compacta that was retrogradely-labeled from the lateral striatum (Supplemental Figure 2). We also saw a few scattered Cbln1-ir but FG-negative cells in pars reticulata. A cluster of Cbln1-ir cells was present in the pars lateralis and peripeduncular area, but these cells were not retrogradely labeled. A small contingent of Cbln1-ir axons was also seen in the peripeduncular region; a very small number of these axons extended ventromedially to traverse the area dorsal to the lateral half of the pars compacta. In

summary, these data suggest that virtually all of the Cbln1 innervation of the lateral striatum is derived from the PF.

Ultrastructural observations on Cbln1-ir in the striatum

In striatal presynaptic elements Cbln1-ir was observed in both pre-terminal axon segments and axon terminals (see Figure 4). In addition, Cbln1-ir was occasionally seen in myelinated axons. Within pre-terminal axons cut in cross section, the reaction product was often found throughout the labeled profile. In the few examples where the preterminal axon was longitudinally sectioned for several microns, patches of label that were separated by unlabeled regions of axon were present. The immunoreactive product in larger terminals usually did not fill the entire profile; Cbln1-ir was seen close to the plasma membrane of the terminal, with DAB reaction product interspersed between the plasma membrane and synaptic vesicles. In some cases, the label was present between the plasma membrane and a mitochondrion in the terminal; these patches of immunoreactivity were on some occasions in close proximity to a presynaptic grid.

In addition to the presynaptic localization of Cbln1-ir, we also observed some Cbln1-immunoreactivity in MSNs, both in dendritic shafts and spines (Fig. 4). In dendritic shafts, patches of DAB reaction product were associated with either the plasma membrane or internal membranous structures. In smaller dendritic spines, label sometimes filled the spine. More frequently, patches of label were observed, sometimes associated with the plasma membrane and occasionally associated with the spine apparatus. The postsynaptic densities (PSDs) of asymmetric synapses on spines and dendrites were frequently so dark they appeared to be labeled. In some cases, these dark PSDs were contiguous with patches of DAB label that extended laterally and/or internally, suggesting that at some synaptic contacts, Cbln1-ir was associated with the postsynaptic specialization. However, because the PSD is so electron dense, it is not possible to state with any certainty if Cbln1 is associated with the PSD.

Effects of genetic deletion of cbln1 on MSN dendrites

We observed a mean 22% increase in MSN dendritic spine density in Golgi-impregnated neurons from *cbln1*$^{-/-}$ relative to wildtype littermate mice ($t_7 = 7.718$, $p = .0001$; see Fig. 5). The total dendritic length of MSNs was the same across genotypes (Fig. 5). All MSN spines in *cbln1* null mutants were < 4.0 μm in length, suggesting that they are not filopodia, and the frequency distributions of spine lengths in Cbln1 knockout and wildtype mice were almost identical (Fig. 5). There was no difference across genotypes in the proportion of total spines that were thin-, stubby-, or mushroom-shaped (Fig. 5).

Stereological assessment revealed that the number of Nissl-stained PF cells did not differ significantly across genotypes (see Figure 6). Consistent with this observation, immunoblot methods did not uncover any differences in striatal VGluT2 levels of *cbln1* knockout and wildtype mice (Figure 6).

Medium spiny neuron synaptic changes in cbln1 knockout mice

Consistent with the increase in spine density in the *cbln1*$^{-/-}$ mice, we observed a 21.7% increase in the frequency of axospinous synapses in the striatal neuropil of the *cbln1* knockout relative to wildtype mouse (2.449 synapses/10 mm^2 for *cbln1*$^{-/-}$ versus 2.013 synapses/10 mm^2 for *cbln1*$^{+/+}$ mice). Thus, although MSN dendritic spine number was increased in *cbln1*$^{-/-}$ mice, these spines were not “naked” but had synaptic partners. Because we examined only two animals of each genotype these values were not statistically different, although a strong trend was uncovered (t=3.599; p=0.069). The relative difference in axospinous synapses across wildtype and *cbln1*$^{-/-}$ mice was not due to larger PSDs in the

knockout mice, which would have rendered axospinous synapses more easily observed in random single sections: mean PSD lengths were 0.236 mm for *cbln1*$^{-/-}$ versus 0.228 mm for wildtype mice. In addition, the incidence of perforated axospinous PSDs did not differ across genotypes (c^2=0.129; p=0.7195).

Discussion

Cbln1 was expressed by PF but not CM thalamostriatal neurons in the mouse and rat. Genetic deletion of *cbln1* increased the density of MSN dendritic spines, with a corresponding increase in the frequency of axospinous synapses on MSNs. These findings offer the first demonstration of extra-cerebellar actions of Cbln1 and indicate that the actions of Cbln1 differ markedly across brain regions.

Localization of Cbln1 in thalamostriatal neurons

Cbln1 was localized to a subset of thalamostriatal projection neurons: thalamostriatal axons originating in the PF but not central medial complex expressed Cbln1-ir. This distribution of Cbln1-ir is consistent with the distribution of *cbln1* mRNA-positive cells in the rodent thalamus (Miura et al., 2006), but differs somewhat from that seen in primates, where Cbln1-ir is present across the intralaminar thalamic nuclei that innervate the striatum, including the centremedian and central medial nuclei as well as the PF (Murray et al., 2007; K. D. Murray, personal communication). Essentially all PF cells in both the mouse and rat express Cbln1, and because all Cbln1-ir cells in the PF also express NeuN-ir, Cbln1 in the PF is localized to neurons but not glia, consistent with the observations of Wei et al. (2007).

The Cbln1 innervation of the striatum appears to be derived almost solely from the PF. *In situ* hybridization histochemistry studies have not observed *cbln*1 mRNA in striatal neurons (Miura et al., 2006). Cbln1-ir processes are seen across the entire striatum but with a clear lateral-to-medial gradient, a pattern consistent with the projection of PF neurons onto the striatum (Berendse and Groenewegen, 1990). Moreover, tracer deposits into the dorsolateral striatum revealed that all PF cells retrogradely-labeled from the striatum expressed Cbln1-ir. In contrast, we did not observe retrograde labeling of Cbln1-ir cortical neurons after tracer deposits into the striatum, consistent with the lack of *cbln1* mRNA or Cbln1-ir in most cortical neurons (Miura et al., 2006; Wei et al., 2007). Although the retrosplenial cortex contains Cbln1-ir cells, our tracer injections into the dorsolateral striatum failed to label cells in this cortical area, consistent with a projection of the retrosplenial cortex to the medial but not lateral striatum (McGeorge and Faull, 1989). Moreover, with the exception of a single Cbln1-ir neuron in the dorsal tier of the substantia nigra, we did not observe any double-labeled cells in the cortex, midbrain, or pons. Thus, it appears that lateral striatal Cbln1-ir afferents almost exclusively originate in the PF. We have not systematically examined the origin of Cbln1 axons in the medial striatum.

We saw very fine Cbln1-ir axons arborizing amidst the dendrites of striatal cells with a soma size characteristic of MSNs. Intracellular LY injections confirmed that MSNs were the primary target of Cbln1-ir inputs. The density of these Cbln1-ir axons is somewhat less than might be expected in light of the abundant expression of *cbln1* mRNA and Cbln1 protein in PF neurons. This may reflect rapid release of Cbln1 from striatal terminals of PF neurons. The storage compartment for release of Cbln1 remains unclear. Wei et al. (2007) found that Cbln1-ir is localized to lysosomes and late-stage endosomes. Although this pattern of localization is typical of proteins targeted for degradation, there are reports of neuronal secretory lysosomes (Arantes & Andrews, 2006; Coggins et al., 2007), which may be storage depots for Cbln1.

Our light microscopic computer-aided reconstructions were consistent with Cbln1-ir axons being apposed to both MSN dendritic spines and shafts. Consistent with these observations, our ultrastructural examination revealed that presynaptic Cbln1-ir terminals synapse predominantly but not exclusively with MSN spines. Lacey et al. (2007) showed that some PF neurons form both axospinous and axodendritic synapses with MSNs, while others predominantly make axospinous synapses. Because all PF neurons express Cbln1, it appears likely that both MSN dendritic spines and shafts are the targets of Cbln-ir axons.

Somewhat surprisingly, our ultrastructural studies also revealed that Cbln1-ir is relatively common in MSNs, particularly in dendritic spines. This finding stands in contrast to the lack of *cbln1* mRNA, as detected by *in situ* hybridization histochemistry or RT-PCR in striatal neurons (Miura et al., 2006), although there are examples of various transcripts not being expressed under basal conditions but becoming apparent after an appropriate challenge (Deutch and Zahm, 1992). Our electron microscopic findings are consistent with recent data of Wei et al. (2009), who showed that Cbln1 is released from cerebellar granule cells and then accumulates in Purkinje cells, i.e., is accumulated by postsynaptic elements after release from Cbln1-containing terminals. Thus, it appears that Cbln1 from thalamostriatal neurons may influence MSNs either by interacting with an as yet un-identified receptor on MSNs, or by being incorporated by striatal cells and then exerting some effect.

Dendritic spine changes and MSN synapses

We observed a marked increase in the density of MSN dendritic spines in *cbln1*$^{-/-}$ mice. Because lateral striatal afferents from sources other than the PF do not express Cbln1, it appears that the increased number of dendritic spines seen in the *cbln1*$^{-/-}$ mouse is due to the loss of Cbln1 in thalamostriatal neurons.

The increased number of dendritic spines was not attributable to an increased number of filopodia, immature spines that are longer than mature spines. Thus, mean spine length and the frequency distributions of spine length were virtually identical across *cbln1* knockout and wildtype mice. In addition, the observation that the proportion of total spines of different morphological classes was the same across genotypes further suggests that the spines that are present on striatal MSNs are mature. At the ultrastructural level we observed no change in the length of the postsynaptic density or the number of perforated axospinous synapses, consistent with a normal synaptic organization with an increased frequency of synaptic contacts.

The increased density of dendritic spines and frequency of axospinous asymmetric synapses in *cbln1*$^{-/-}$ mice runs counter to findings in the cerebellar cortex of *cbln1* knockout mice, where there is no change in Purkinje cell dendritic spine density but the majority of spines lack a presynaptic partner (Hirai et al., 2005; Ito-Ishida et al., 2008). In addition, while there is no change in PSD length in the supernumerary MSN spines of *cbln1*$^{-/-}$ mice, PSDs are enlarged at the pf-PC synapses of these mutant mice. These contrasting regionally-specific changes in synaptic organization in *cbln1* null mutant mice raise the possibility that different Cbln1 receptors or intracellular signaling cascades may subserve different effects on postsynaptic neurons. Alternatively, Cbln1 released from PF axons and then incorporated into MSNs directly or in association with internalization of a G protein-coupled receptor may modify the structures of MSNs.

The mechanism through which loss of Cbln1 results in increases in MSN spine density and axospinous synapses is unclear. Our stereological data indicate that the number of PF neurons is not changed in the *cbln1* knockout mouse, and striatal levels of VGluT2 are unchanged in total homogenates of the striatum, consistent with an intact glutamatergic projection of the PF to the striatum in the *cbln1*$^{-/-}$ mouse.

Cbln1 receptors have yet to be identified, although a recent study indicates that upon release of Cbln1 from cerebellar granule cells Cbln1 hexamers bind to PC dendrites (Matsuda et al., 2009). Because glutamate signaling is a key regulator of spine development and maintenance (McKinney et al., 1999; Shi et al., 1999; Lippman and Dunaevsky, 2005; Richards et al, 2005; Alvarez and Sabatini, 2007) and thalamostriatal neurons are glutamatergic, it is possible that Cbln1 signals through a glutamate receptor to change the dendritic structure of MSNs. Hirai et al. (2005) found that the cerebellar phenotype of mice lacking the orphan glutamate receptor *grid2* is similar to that of the *cbln1*$^{-/-}$ mouse, including loss of pf-PC synapses, and proposed that Cbln1 and grid2 are part of the same signaling pathway. Although grid2 does not bind recombinant Cbln1 (unpublished observations), the two are co-clustered at the pf-PC synapse (Miura et al., 2009), leaving open the possibility that grid2 is a subunit of the Cbln1 receptor. However, neither grid2 nor its interacting protein are expressed in the PF or striatum (Gong et al., 2003), suggesting that Cbln1 may signal through unidentified receptor(s) on MSNs to increase spine density. Exploiting the different responses of the cerebellar cortex and striatum to Cbln1 may prove useful in attempts to identify a family of cerebellin receptors.

Functional implications

The density of MSN dendritic spines is changed by a number of different stimuli. In particular, modulation of striatal dopaminergic tone alters spine density, with increases in striatal dopamine eliciting an increase in MSN spine density and depletion of striatal dopamine decreasing spine number (Li et al 2003; Day et al., 2006; Deutch et al., 2007; Meyer et al., 2008). For example, in Parkinson's Disease there is a loss of MSN dendritic spines (Stephens et al., 2005; Zaja-Milatovic et al., 2005), while animals treated chronically with psychostimulants show an increase in MSN spine density (Li et al., 2003).

Interestingly, the cerebellin hexadecapeptide has been shown to elicit catecholamine release both *in vitro* and in perfused adrenal glands *in situ* (Mazzocchi et al, 1999; Albertin et al, 2000). It is possible that the loss of Cbln1 modifies striatal dopamine tone and thereby increases dendritic spine density. The PF has been reported to send a small projection to the SN (Marini et al. 1999). However, we found little Cbln1-ir in the SN, with some Cbln1-ir axons in the pars lateralis. This suggests that Cbln1 is unlikely to regulate striatal MSNs by means of altered function of PF projections to the SN. An alternative scenario is that Cbln1 acts on heteroceptors localized to the axon terminals of nigrostriatal neurons to modulate dopamine release and thereby decrease MSN dendritic spine density. Consistent with this speculation is the finding of Kilpatrick et al. (1986), who noted that lesions of the PF increase the density of striatal dopamine D2 receptors, a change that would be expected to increase dendritic spine density in the face of normal or increased striatal dopamine tone.

Recent studies have suggested that modifying the activity of thalamostriatal neurons may lead to symptomatic improvement in PD. Caparros-Lefebvre et al. (1994), in an evaluation of the effects of deep brain stimulation (DBS) of the motor thalamus on PD symptoms, suggested that electrode placements that involved the CM-PF yielded the best responses. Several recent small clinical trials of CM-PF DBS in PD have been conducted, concluding that stimulation of the CM-PF improves extrapyramidal motor symptoms, including tremor, and decreases levodopa-induced abnormal involuntary movements (Caparros-Lefebvre et al, 1999; Peppe et al., 2008; Benabid, 2009; Stefani et al., 2009). While the mechanism of action of DBS remains unclear, a functional inhibition of the stimulated site is a leading hypothesis to account for the therapeutic effects of DBS.

Experimental animal data are consistent with the data from the CM-PF DBS studies and suggest that disruption of thalamostriatal projections may reverse dopamine depletion-induced changes in striatal function (Bacci et al., 2004). Similarly, DBS of the PF in rats

with 6-hydroxydopamine lesions of the nigrostriatal neurons attenuates the increase in striatal preproenkephalin but not preprotachykinin mRNA that is seen after dopamine depletion and improves motor performance (Kerkerian-Le Goff et al., 2009). These data suggest that the PF may modulate the deleterious effects of striatal dopamine depletion on indirect pathway MSNs.

Taken together, these data suggest that decreased thalamostriatal drive may counteract the effects of dopamine loss on MSNs. Interestingly, in Parkinson's Disease the numbers of PF and CM neurons is decreased by almost half (Henderson et al., 2000), suggesting that loss of thalamostriatal neurons in PD may be a compensatory response to striatal dopamine denervation. Our observation that loss of Cbln1 leads to increased numbers of MSN dendritic spines suggests that modulating thalamostriatal Cbln1 may be a novel means of improving symptoms or slowing progression in Parkinson's Disease.

Supplementary Material

Refer to Web version on PubMed Central for supplementary material.

Acknowledgments

The authors gratefully acknowledge the help of Mr. Peter Vollbrecht, Dr. Hui-Dong Wang, and Dr. Michael Bubser with various aspects of the experiments, the expert technical assistance of Murat Senyuz, and the comments of Dr. Karl Murray, who shared with us his data on Cbln1 expression in the primate thalamus.

This work was supported by National Institutes of Health [F31 NS061528 to SVK; R01 RR00165 to ECM; CA21765, NS042828, and NS051537 to JIM; PO1 NS44282 and RO1MH-077298 to AYD], a Merit Award from the Department of Veterans Affairs to ECM; American Lebanese Syrian Associated Charities to JIM; and the National Parkinson Foundation Center of Excellence at Vanderbilt to AYD. The content is solely the responsibility of the authors and does not necessarily represent the official views of the NINDS or NCI of the National Institutes of Health, the Department of Veterans Affairs, or the National Parkinson Foundation.

References

Albertin G, Malendowicz LK, Macchi C, Markowska A, Nussdorfer GG. Cerebellin stimulates the secretory activity of the rat adrenal gland: in vitro and in vivo studies. Neuropeptides. 2000; 34:7–11. [PubMed: 10688962]

Aldridge GM, Podrebarac DM, Greenough WT, Weiler IJ. The use of total protein stains as loading controls: an alternative to high-abundance single-protein controls in semi-quantitative immunoblotting. J Neurosci Methods. 2008; 172:250–4. [PubMed: 18571732]

Alvarez VA, Sabatini BL. Anatomical and physiological plasticity of dendritic spines. Ann Rev Neurosci. 2007; 30:79–97. [PubMed: 17280523]

Arantes RM, Andrews NW. A role for synaptotagmin VII-regulated exoctyosis of lysosomes in neurite outgrowth from primary sympathetic neurons. J Neurosci. 2006; 26:4630–7. [PubMed: 16641243]

Bacci JJ, Kachidian P, Kerkerian-Le Goff L, Salin P. Intralaminar thalamic nuclei lesions: widespread impact on dopamine denervation-mediated cellular defects in the rat basal ganglia. J Neuropathol Exp Neurol. 2004; 63:20–31. [PubMed: 14748558]

Bao D, Pang Z, Morgan JI. The structure and proteolytic processing of Cbln1 complexes. J Neurochem. 2005; 95:618–29. [PubMed: 16135095]

Bao D, Pang Z, Morgan MA, Parris J, Rong Y, Li L, Morgan JI. Cbln1 is essential for interaction-dependent secretion of Cbln3. Mol Cell Biol. 2006; 26:9327–37. [PubMed: 17030622]

Benabid AL. Targeting the caudal intralaminar nuclei for functional neurosurgery of movement disorders. Brain Res Bull. 2009; 78:109–112. [PubMed: 18812212]

Berendse HW, Groenewegen HJ. Organization of the thalamostriatal projections in the rat, with special emphasis on the ventral striatum. J Comp Neurol. 1990; 299:187–228. [PubMed: 2172326]

Bubser M, Scruggs JL, Young CD, Deutch AY. The distribution and origin of the calretinin-containing innervation of the nucleus accumbens of the rat. Eur J Neurosci. 2000; 12:1591–1598. [PubMed: 10792437]

Caparros-Lefebvre D, Ruchoux MM, Blond S, Petit H, Percheron G. Long-term thalamic stimulation in Parkinson's disease: postmortem anatomoclinical study. Neurology. 1994; 44:1856–1860. [PubMed: 7936236]

Caparros-Lefebvre D, Blond S, Feltin MP, Pollak P, Benabid AL. Improvement of levodopa induced dyskinesias by thalamic deep brain stimulation is related to slight variation in electrode placement: possible involvement of the centre median and parafascicularis complex. J Neurol Neurosurg Psychiatry. 1999; 67:308–314. [PubMed: 10449551]

Coggins MR, Grabner CP, Almers W, Zenisek D. Stimulated exocytosis of endosomes in goldfish retinal bipolar neurons. J Physiol. 2007; 584(Pt 3):853–65. [PubMed: 17823206]

Day M, Wang Z, Ding J, An X, Ingham CA, Shering AF, Wokosin D, Ilijic E, Sun Z, Sampson AR, Mugnaini E, Deutch AY, Sesack SR, Arbuthnott GW, Surmeier DJ. Selective elimination of glutamatergic synapses on striatopallidal neurons in Parkinson disease models. Nat Neurosci. 2006; 9:251–9. [PubMed: 16415865]

Deutch AY, Zahm DS. The current status of neurotensin-dopamine interactions: issues and speculations. Ann N Acad Sci. 1992; 668:232–252.

Deutch AY, Colbran RJ, Winder DJ. Striatal plasticity and medium spiny neuron dendritic remodeling in parkinsonism. Parkinsonism Relat Disord. 2007; 13:S251–8. [PubMed: 18267246]

Ding J, Peterson JD, Surmeier DJ. Corticostriatal and thalamostriatal synapses have distinctive properties. J Neurosci. 2008; 28:6483–92. [PubMed: 18562619]

Dubé L, Smith AD, Bolam JP. Identification of synaptic terminals of thalamic or cortical origin in contact with distinct medium-size spiny neurons in the rat neostriatum. J Comp Neurol. 1988; 267:455–71. [PubMed: 3346370]

Fujiyama F, Unzai T, Nakamura K, Nomura S, Kaneko T. Difference in organization of corticostriatal and thalamostriatal synapses between patch and matrix compartments of rat neostriatum. Eur J Neurosci. 2006; 24:2813–24. [PubMed: 17156206]

Giménez-Amaya JM, de las Heras S, Erro E, Mengual E, Lanciego JL. Considerations on the thalamostriatal system with some functional implications. Histol Histopathol. 2000; 15:1285–92. [PubMed: 11005252]

Gong S, Zheng C, Doughty ML, Losos K, Didkovsky N, Schambra UB, Nowak NJ, Joyner A, Leblanc G, Hatten ME, Heintz N. A gene expression atlas of the central nervous system based on bacterial artificial chromosomes. Nature. 2003; 425:917–25. [PubMed: 14586460]

Henderson JM, Carpenter K, Cartwright H, Halliday GM. Degeneration of the centre median-parafascicular complex in Parkinson's disease. Ann Neurol. 2000; 47:345–352. [PubMed: 10716254]

Hirai H, Pang Z, Bao D, Miyazaki T, Li L, Miura E, Parris J, Rong Y, Watanabe M, Yuzaki M, Morgan JI. Cbln1 is essential for synaptic integrity and plasticity in the cerebellum. Nat Neurosci. 2005; 8:1534–41. [PubMed: 16234806]

Ito-Ishida A, Miura E, Emi K, Matsuda K, Iijima T, Kondo T, Kohda K, Watanabe M, Yuzaki. Cbln1 regulates rapid formation and maintenance of excitatory synapses in mature cerebellar Purkinje cells in vitro and in vivo. J Neurosci. 2008; 28:5920–30. [PubMed: 18524896]

Kaneko T, Fujiyama F, Hioki H. Immunohistochemical localization of candidates for vesicular glutamate transporters in the rat brain. J Comp Neurol. 2002; 444:39–62. [PubMed: 11835181]

Kerkerian-Le Goff L, Bacci JJ, Jouve L, Melon C, Salin P. Impact of surgery targeting the caudal intralaminar thalamic nuclei on the pathophysiological functioning of basal ganglia in a rat model of Parkinson's disease. Brain Res Bull. 2009; 78:80–84. [PubMed: 18790021]

Kilpatrick IC, Jones MW, Pycock CJ, Riches I, Phillipson OT. Thalamic control of dopaminergic functions in the caudate-putamen of the rat--III. The effects of lesions in the parafascicular-intralaminar nuclei on D2 dopamine receptors and high affinity dopamine uptake. Neurosci. 1986; 19:991–1005.

Lacey CJ, Bolam JP, Magill PJ. Novel and distinct operational principles of intralaminar thalamic neurons and their striatal projections. J Neurosci. 2007; 27:4374–84. [PubMed: 17442822]

Lanciego JL, López IP, Rico AJ, Aymerich MS, Pérez-Manso M, Conte L, Combarro C, Roda E, Molina C, Gonzalo N, Castle M, Tuñón T, Erro E, Barroso-Chinea P. The search for a role of the caudal intralaminar nuclei in the pathophysiology of Parkinson's disease. Brain Res Bull. 2009; 78:55–9. [PubMed: 18790023]

Lapper SR, Bolam JP. Input from the frontal cortex and the parafascicular nucleus to cholinergic interneurons in the dorsal striatum of the rat. Neurosci. 1992; 51:533–45.

Li Y, Kolb B, Robinson TE. The location of persistent amphetamine-induced changes in the density of dendritic spines on medium spiny neurons in the nucleus accumbens and caudate-putamen. Neuropsychopharmacol. 2003; 28:1082–5.

Lippman J, Dunaevsky A. Dendritic spine morphogenesis and plasticity. J Neurobiol. 2005; 64:47–57. [PubMed: 15884005]

Marini G, Pianica L, Tredici G. Descending projections arising from the parafascicular nucleus in rats: trajectory of fibers, projection pattern and mapping of terminations. Somatosens Mot Res. 1999; 16:207–22. [PubMed: 10527369]

Mathur BN, Caprioli RM, Deutch AY. Proteomic analysis illuminates a novel structural definition of the claustrum and insula. Cereb Cortex. 2009; 19:2372–9. [PubMed: 19168664]

Matsuda K, Kondo T, Iijima T, Matsuda S, Watanabe M, Yuzaki M. Cbln1 binds to specific postsynaptic sites at parallel fiber-Purkinje cell synapses in the cerebellum. Eur J Neurosci. 2009; 29:707–717. [PubMed: 19200061]

Matsumoto N, Minamimoto T, Graybiel AM, Kimura M. Neurons in the thalamic CM-Pf complex supply striatal neurons with information about behaviorally significant sensory events. J Neurophysiol. 2001; 85:960–76. [PubMed: 11160526]

Mazzocchi G, Andreis PG, De Caro R, Aragona F, Gottardo L, Nussdorfer GG. Cerebellin enhances in vitro secretory activity of human adrenal gland. J Clin Endocrinol Metab. 1999; 84:632–5. [PubMed: 10022429]

McGeorge AJ, Faull RL. The organization of the projection from the cerebral cortex to the striatum in the rat. Neurosci. 1989; 29:503–37.

McKinney RA, Capogna M, Dürr R, Gähwiler BH, Thompson SM. Miniature synaptic events maintain dendritic spines via AMPA receptor activation. Nat Neurosci. 1999; 2:44–9. [PubMed: 10195179]

Meyer DA, Richer E, Benkovic SA, Hayashi K, Kansy JW, Hale CF, Moy LY, Kim Y, O'Callaghan JP, Tsai LH, Greengard P, Nairn AC, Cowan CW, Miller DB, Antich P, Bibb JA. Striatal dysregulation of Cdk5 alters locomotor responses to cocaine, motor learning, and dendritic morphology. Proc Natl Acad Sci USA. 2008; 105:18561–6. [PubMed: 19017804]

Minamimoto T, Hori Y, Kimura M. Roles of the thalamic CM-PF complex-Basal ganglia circuit in externally driven rebias of action. Brain Res Bull. 2009; 78:75–9. [PubMed: 18793702]

Minamimoto T, Kimura M. Participation of the thalamic CM-Pf complex in attentional orienting. J Neurophysiol. 2002; 87:3090–101. [PubMed: 12037210]

Miura E, Iijima T, Yuzaki M, Watanabe M. Distinct expression of Cbln family mRNAs in developing and adult mouse brains. Eur J Neurosci. 2006; 24:750–60. [PubMed: 16930405]

Miura E, Matsuda K, Morgan JI, Yuzaki M, Watanabe M. Cbln1 accumulates and colocalizes with Cbln3 and GluRdelta2 at parallel fiber-Purkinje cell synapses in the mouse cerebellum. Eur J Neurosci. 2009; 29:693–706. [PubMed: 19250438]

Mugnaini E, Morgan JI. The neuropeptide cerebellin is a marker for two similar neuronal circuits in rat brain. Proc Natl Acad Sci U S A. 1987; 84:8692–6. [PubMed: 3317418]

Mullen RJ, Buck CR, Smith AM. NeuN, a neuronal specific nuclear protein in vertebrates. Development. 1992; 116:201–11. [PubMed: 1483388]

Muly EC, Maddox M, Smith Y. Distribution of mGluR1alpha and mGluR5 immunolabeling in primate prefrontal cortex. J Comp Neurol. 2003; 467:521–35. [PubMed: 14624486]

Murray KD, Choudary PV, Jones EG. Nucleus- and cell-specific gene expression in monkey thalamus. Proc Natl Acad Sci USA. 2007; 104:1989–94. [PubMed: 17261798]

Pakan JM, Graham DJ, Iwaniuk AN, Wylie DR. Differential projections from the vestibular nuclei to the flocculus and uvula-nodulus in pigeons (Columba livia). J Comp Neurol. 2008; 508:402–17. [PubMed: 18335537]

Pang Z, Zuo J, Morgan JI. Cbln3, a novel member of the precerebellin family that binds specifically to Cbln1. J Neurosci. 2000; 20:6333–9. [PubMed: 10964938]

Peppe A, Gasbarra A, Stefani A, Chiavalon C, Pierantozzi M, Fermi E, Stanzione P, Caltagirone C, Mazzone P. Deep brain stimulation of CM/PF of thalamus could be the new elective target for tremor in advanced Parkinson's Disease? Parkinsonism Relat Disord. 2008; 14:501–504. [PubMed: 18337153]

Peters A, Kaiserman-Abramof IR. The small pyramidal neuron of the rat cerebral cortex. The perikaryon, dendrites and spines. Am J Anat. 1970; 127:321–55. [PubMed: 4985058]

Richards DA, Mateos JM, Hugel S, de Paola V, Caroni P, Gähwiler BH, McKinney RA. Glutamate induces the rapid formation of spine head protrusions in hippocampal slice cultures. Proc Natl Acad Sci USA. 2005; 102:6166–71. [PubMed: 15831587]

Sadikot AF, Parent A, Smith Y, Bolam JP. Efferent connections of the centromedian and parafascicular thalamic nuclei in the squirrel monkey: a light and electron microscopic study of the thalamostriatal projection in relation to striatal heterogeneity. J Comp Neurol. 1992; 320:228–42. [PubMed: 1619051]

Shi SH, Hayashi Y, Petralia RS, Zaman SH, Wenthold RJ, Svoboda K, Malinow R. Rapid spine delivery and redistribution of AMPA receptors after synaptic NMDA receptor activation. Science. 1999; 284:1811–6. [PubMed: 10364548]

Slemmon JR, Blacher R, Danho W, Hempstead JL, Morgan JI. Isolation and sequencing of two cerebellum-specific peptides. Proc Natl Acad Sci U S A. 1984; 81:6866–6870. [PubMed: 16593526]

Smeal RM, Keefe KA, Wilcox KS. Differences in excitatory transmission between thalamic and cortical afferents to single spiny efferent neurons of rat dorsal striatum. Eur J Neurosci. 2008; 28:2041–52. [PubMed: 19046385]

Smith Y, Raju DV, Pare JF, Sidibe M. The thalamostriatal system: a highly specific network of the basal ganglia circuitry. Trends Neurosci. 2004; 27:520–7. [PubMed: 15331233]

Smith Y, Raju D, Nanda B, Pare JF, Galvan A, Wichmann T. The thalamostriatal systems: anatomical and functional organization in normal and parkinsonian states. Brain Res Bull. 2009; 78:60–8. [PubMed: 18805468]

Stefani A, Peppe A, Pierantozzi M, Galati S, Moschella V, Stanzione P, Mazzone P. Multi-target strategy for Parkinsonian patients: the role of deep brain stimulation in the centromedian-parafascicularis complex. Brain Res Bull. 2009; 78:113–118. [PubMed: 18812214]

Stephens B, Mueller AJ, Shering AF, Hood SH, Taggart P, Arbuthnott GW, Bell JE, Kilford L, Kingsbury AE, Daniel SE, Ingham CA. Evidence of a breakdown of corticostriatal connections in Parkinson's disease. Neuroscience. 2005; 132:741–754. [PubMed: 15837135]

Stocker SD, Simmons JR, Stornetta RL, Toney GM, Guyenet PG. Water deprivation activates a glutamatergic projection from the hypothalamic paraventricular nucleus to the rostral ventrolateral medulla. J Comp Neurol. 2006; 494:673–685. [PubMed: 16374796]

Urade Y, Oberdick J, Molinar-Rode R, Morgan JI. Precerebellin is a cerebellum-specific protein with similarity to the globular domain of complement C1q B chain. Proc Natl Acad Sci USA. 1991; 88:1069–73. [PubMed: 1704129]

Wei P, Smeyne RJ, Bao D, Parris J, Morgan JI. Mapping of Cbln1-like immunoreactivity in adult and developing mouse brain and its localization to the endolysosomal compartment of neurons. Eur J Neurosci. 2007; 26(10):2962–78. [PubMed: 18001291]

Wei P, Rong Y, Li L, Bao D, Morgan JI. Characterization of trans-neuronal trafficking of Cbln1. Mol Cell Neurosci. 2009; 41:258–73. [PubMed: 19344768]

Zaja-Milatovic S, Milatovic D, Schantz AM, Zhang J, Montine KS, Samii A, Deutch AY, Montine TJ. Dendritic degeneration in neostriatal medium spiny neurons in Parkinson disease. Neurology. 2005; 64:545–547. [PubMed: 15699393]

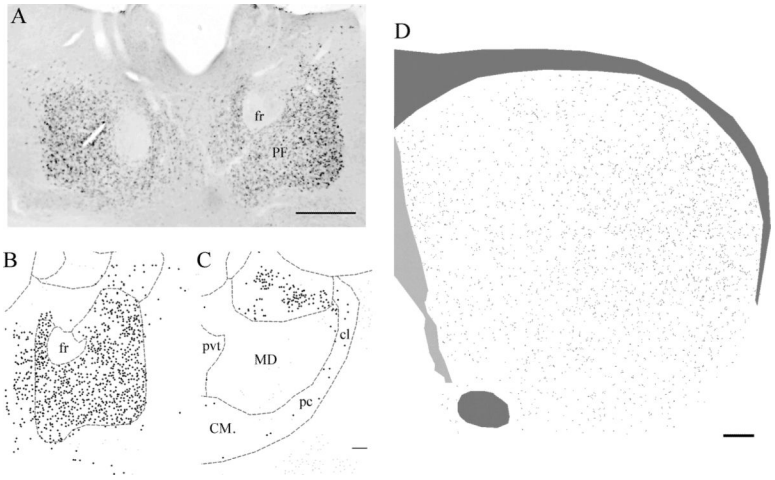

Figure 1.

A) Cbln1 immunoreactivity in cells of the PF. Cbln1-ir cells are seen throughout the PF. **B–C)** Chartings of the distribution of Cbln1-ir neurons in the PF (B) and in the CM complex (panel C). In contrast to the PF, only rare cells in the CM complex, including centrolateral, paracentral, and central medial nuclei, express Cbln1-ir. ***D)*** Charting of the distribution of Cbln1-ir axons in the striatum. Cbln1-ir axons are seen throughout the striatum, but with a clear mediolateral gradient in their density. Abbreviations: CM, central medial complex; cl, centrolateral division of CM; pc, paracentral division of CM; fr, fasciculus retroflexus; MD, mediodorsal nucleus of the thalamus; pvt, paraventricular thalamic nucleus. Scale bar panel ***A***, 200 μm; ***B***, ***C*** 100 μm; ***D***, 100 μm.

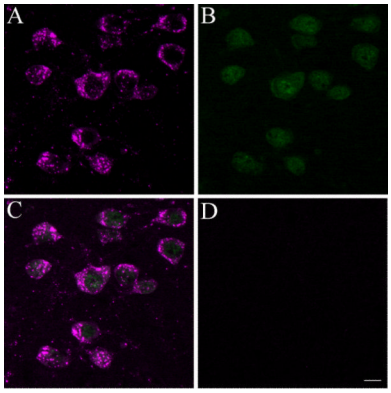

Figure 2.

Cbln1-ir is expressed in neurons of the PF. ***A–C)*** Cbln1-ir cells (shown in magenta) in the PF (panel A) also express the neuronal marker NeuN (shown in green in panel B), with the merged image shown in C. ***D***, No Cbln1-ir is seen in the PF of the *cbln1* knockout mouse. Scale bar, 10 μm.

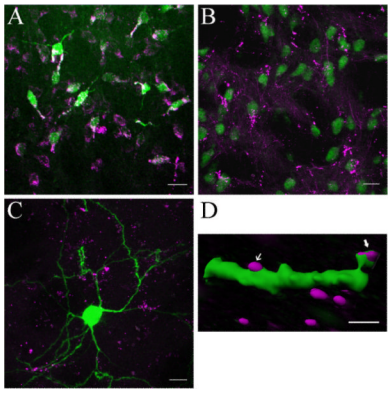

Figure 3.

A) PF neurons were retrogradely-labeled from the striatum with FluoroGold (green). All retrogradely-labeled FG cells expressed Cbln1-ir (magenta), although some Cbln1-ir cells, seen toward the bottom of the panel, were not retrogradely-labeled. ***B)*** Fine-caliber Cbln1-ir axons (magenta) are present in the striatum, with profuse terminal plexi that appear to be apposed to the dendrites and somata of striatal NeuN-ir neurons (green). ***C,D)*** Relationship of Cbln1-ir axons (magenta) to Lucifer Yellow-filled MSNs (green). In panel C a merged confocal image shows that Cbln1-ir axons are interspersed among the dendrites of MSNs. Panel D shows an Imaris reconstruction of a confocal image revealing Cbln1-ir appositions onto both a spine head and the dendritic shaft of a distal MSN dendrite. Scale bars: A, B, 20 μm; C, 10 μm; D) 2.0 μm.

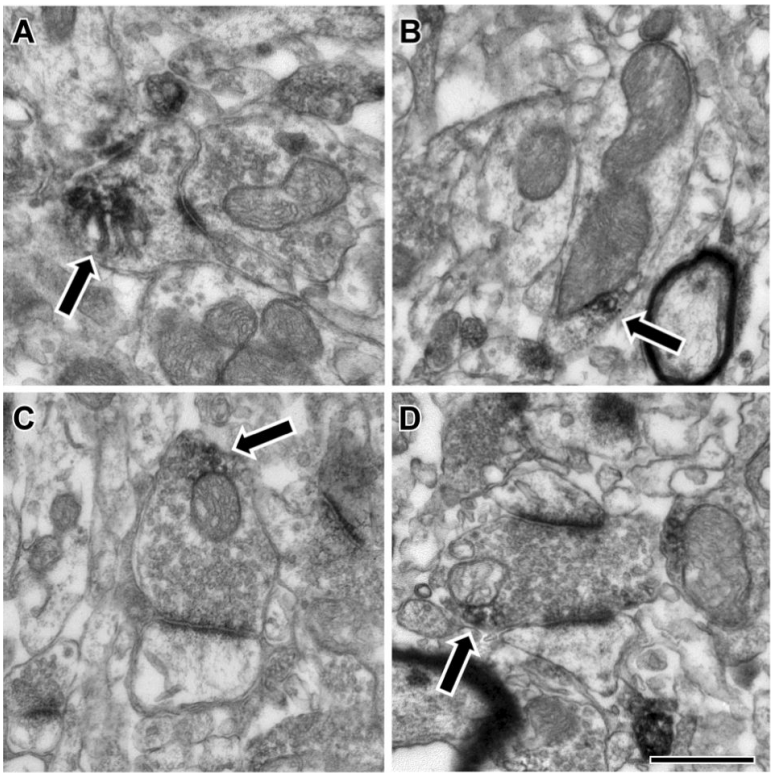

Figure 4.

Electron microscopic localization of Cbln1 immunoreactivity in the rat striatum. Cbln1-ir (arrows) was found in many different subcellular compartments in the striatum, including axon terminals and dendrites. **A)** Within spines, Cbln1-ir was occasionally associated with the spine apparatus. **B)** In dendrites, Cbln1-ir was often observed adjacent to mitochondria, though other small vesicular structures were also seen nearby. **C, D)** Within axon terminals, Cbln1-ir was also often observed near mitochondria or vesicles in close proximity to the mitochondria. Synaptic contacts made by labeled terminals were always asymmetric and targeted both spines (panel C) and dendrites (D). Scale bar represents 500 nm in A, C, and D; and 600 nm in B.

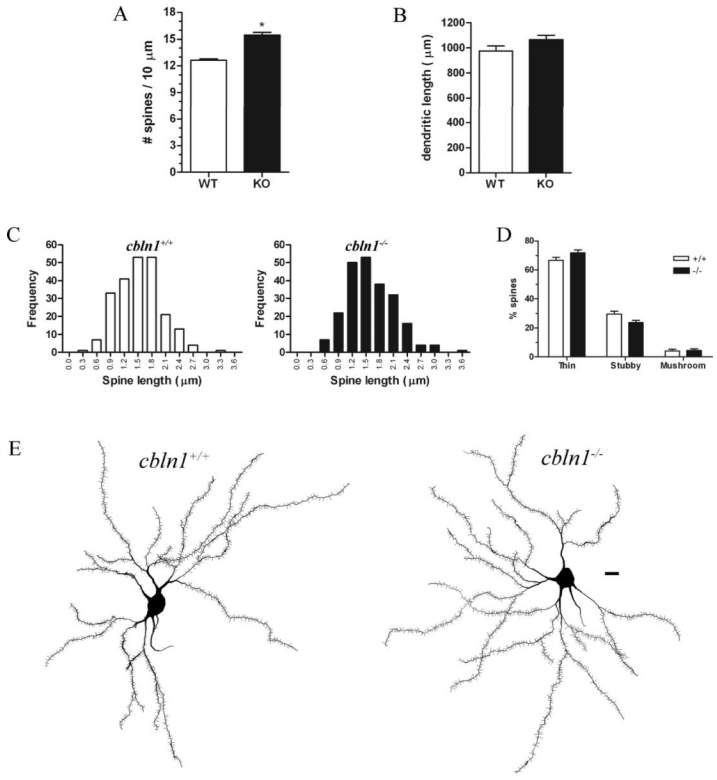

Figure 5.

MSN dendritic spine density is increased in *cbln1*$^{-/-}$ mice. ***A)*** Dendritic spine density is increased in the *cbln1* knockout (KO) relative to wildtype (WT) mice. ***B)*** Total dendritic length of MSNs does not differ across genotypes. **C)** The frequency distributions of the length of MSN spines are not significantly different across *cbln1*$^{+/+}$ and cbln1$^{-/-}$ mice. Moreover, none of the spines has a length corresponding to that of filopodia (> 4.5 μm). ***D)*** No differences in the proportions of thin, stubby, or mushroom-shaped MSN spines were observed across genotypes. ***E)*** Neurolucida reconstructions of Golgi-impregnated MSNs from *cbln1*$^{+/+}$ (left) and *cbln1*$^{-/-}$ (right) mice. Scale bar, 10 μm.

*p ≤ .0001

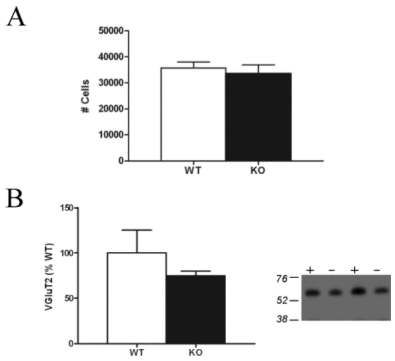

Figure 6.

A) There is no difference in the number of PF neurons in *cbln1* knockout (KO) and wildtype (WT) mice, as revealed by sterological assessment. ***B)*** Striatal VGluT2 levels, as revealed by a single band at ~66 kDa on immunoblots, are not significantly different in *cbln1* KO (−) and WT (+) mice.

Table 1

Primary Antibodies

Antigen	Immunogen	Source	Manufacturer	Dilution
Cbln1	Synthetic peptide (amino acids 95–112 of mouse Cbln1), conjugated to keyhole limpet hemocyanin (KLH); affinity purified with the same peptide (Bao et al. 2005)	Rabbit, Polyclonal	James I. Morgan	1:600 (immunofluorescence) 1:1000 (electron microscopy) 1:2000 (immunoperoxidase)
Cholera toxin B	Cholera toxin B subunit	Goat, polyclonal	List Biological (Campbell, CA), #703	1:5000
NeuN	Purified cell nuclei from mouse brain	Mouse, monoclonal	Millipore (Billerica, MA), #MAB377	1:500
VGluT2	Amino acids 569–582 of rat VGluT2 coupled to KLH	Rabbit, polyclonal	MAb Technologies (Stone Mountain, GA), # VGT2–3	1:4000